J Biosci (2020)45:43
DOI: 10.1007/s12038-020-0011-3

Quinacrine causes apoptosis in human cancer cell lines through caspase-mediated pathway and regulation of small-GTPase

ANGELA SAMANTA[1], GEETHANJALI RAVINDRAN[2] and ANGSHUMAN SARKAR[1]*

[1]*CMBL, Department of Biological Sciences, BITS Pilani K K Birla Goa Campus, Zuarinagar 403 726, India*

[2]*Centre for Cellular and Molecular Biology, Habsiguda, Uppal Road, Hyderabad 500 007, India*

**Corresponding author (Email, asarkar@goa.bits-pilani.ac.in)*

MS received 14 July 2019; accepted 1 January 2020

Quinacrine (QC), an FDA-approved anti-malarial drug, has shown to have anticancer activities. Due to its 'shotgun' nature, QC has become an inevitable candidate for combination chemotherapy. There is lack of study of the molecular interplay between colorectal cancer (CRC) microenvironment and its metastasis. In this study, we focused on the differential anti-cancerous effect of QC on two different human cancer cell lines, HCT 116 and INT 407. Results suggest that cytotoxicity increased in both the cell lines with an increase in QC concentration. The expression patterns of small-GTPases and caspases were altered significantly in QC-treated cells compared to non-treated cells. HSP70 and p53 showed comparable differences in the expression pattern. The wound-healing assay showed an increase in the denuded zone, with an increase in the concentration of QC. The formation of apoptotic nuclei increased with a rise in the concentration of QC in both the cell lines. The decrease and increase in caspase 9 and caspase 3 expression respectively were studied, confirming apoptosis by the extrinsic pathway.

Keywords. Caspase 3; caspase 8; caspase 9; HCT 116; Hsp70; INT 407; p53; Quinacrine; small GTPases

1. Introduction

In India, colorectal cancer (CRC) is the third most common cancer diagnosed in both men and women ('Global cancer statistics'). Detecting the signs of colon cancer and nipping colon cancer in the bud increases the patient's survival rate (Jemal *et al.* 2011). The Asia Pacific region has more instances of CRC, and the mortality rates were seen to have increased in regions of Japan and Singapore. CRC accounts for 10 to 15% of all cancers and is the second leading cause of cancer-related death in industrialized countries (Torres *et al.* 2013); 8–10% of global population is affected by common digestive system diseases which are known as intestine ulcers or gastric ulcers which represents up to 500,000 individuals every year in US (de Lira Mota et al. 2009).

Quinacrine (QC), a derivative of 9 amino-acridine, is an anti-inflammatory molecule that has been used for the treatment of malaria, amebiasis, and giardia and rheumatoid disease (Gurova *et al.* 2005; Wiezorek *et al.* 2010). The antitumor property was observed in both *in vitro* as well as *in vivo* studies (Chowdhury et al. 2006; Ashkenazi 2008). QC's anticancer property was proved in many types of tumor cells (Ortega and Adam 1997; Moghaddam *et al.* 2005). It was reported that QC could activate p53 without genotoxicity through protein stabilization by blocking p53 ubiquitination. This deregulation results from the phosphoinositol-3 kinase/AKT/mammalian target of rapamycin pathways (Fasanmade *et al.* 2001). QC has been shown to bind and inhibit proteins involved in multidrug resistance, disrupting the arachidonic acid pathway, as well as affecting the p53, NF-κB, and AKT pathways (Ehsanian *et al.* 2011).

QC offers anticancer potential by downregulating cellular inhibitor of apoptosis protein-1, and

Published online: 18 February 2020

upregulation of Bax, and cleaved caspase 3 independent of p53 (Sander *et al.* 1998). It is reported that QC activates p53, a transcription factor for cell cycle arrest, cell proliferation control, DNA repair, and apoptosis (Friedl and Wolf 2003). Some pathways mediate p53-induced apoptosis, and one of these involves the Bcl-2 and Bax proteins (Fritz *et al.* 1999; Lozano *et al.* 2003). p53 can interact with Bax by promoting its activation and insertion into the mitochondrial membrane (Sarkar *et al.* 2007). Small GTPases use GDP/GTP (Guanosine diphosphate and Guanosine triphosphate) alternation to actuate a variety of functional switches that are pivotal for cell dynamics. Rho family proteins regulate diverse cellular functions, including proliferation, differentiation, migration, and polarity (Paul-Samojedny *et al.* 2005). Scientists all over the world are trying to search for a chemical/compound, which may affect the regulation of small GTPases, which in turn could play a crucial role in combating oncogenesis. Pathways leading to apoptosis involves different proteins both for the intrinsic and extrinsic pathway. The Bcl-2 family, which constitutes 'intrinsic' pathway, consists of both Bax, which promotes cytochrome c from mitochondria activating caspase 3 (Jin and El-deiry 2005; van Hengel *et al.* 2008).

On the other hand, in the 'extrinsic' pathway, activation of the caspase 8 pathway was reported (Kominami *et al.* 2012). Once activated, caspase 9 or 8 (10) activates downstream 'effector caspases,' which trigger cellular destruction by cleaving several hundred cellular proteins (Cheng *et al.* 2019). Continued research for gaining insights into the mechanisms of action of QC is required for establishing therapeutic methods that might ultimately help to reduce the toxic side effects of drugs. Because of its 9-aminoacridine structure, the anticancer potency of QC has been intensively evaluated in different tumor cells (Ehsanian *et al.* 2011), whereas little is known about the effect of QC in the regulation of small GTPase in human colon cancer and gastric ulcers.

2. Materials and methods

All general laboratory chemicals were purchased from Sigma Aldrich (USA), Life technologies GIBCO BRL (USA), or HIMEDIA (India). HCT 116 cells & INT 407 cells were obtained from the National Centre for Cell Science (NCCS), Pune, India. Culture plastic wares were procured from Corning Life Science. All experiments were carried out in triplicates. Cells were checked for mycoplasma contamination, and it was found negative.

2.1 *In vitro culture of HCT 116 cells & INT 407 cells*

Cells were maintained in Dulbecco's Modified Eagle's Medium (GIBCO) containing 10% Fetal Bovine Serum (Sigma) supplemented with 0.1% antibiotic-antimycotic solution in humidified 5% CO_2 condition at 37°C (van Hengel *et al.* 2008; Cheng *et al.* 2019).

2.2 *Quinacrine (QC)*

Quinacrine dihydrochloride (6-Chloro-9-(4-diethylamino-1-methyl butyl amino)-2-methoxyacridine dihydrochloride, Atebrin dihydrochloride, Mepacrine dihydrochloride; SIGMA -ALDRICH Catalogue No. Q3251) stock (1 mM) was prepared in DMEM. Freshly grown cells were plated at 5×10^4 cells/ml and were exposed to different concentrations of QC.

2.3 *Cell viability*

Cell viability was determined using a hemocytometer (Tiefe Depth Profondeur, Marienfeld, Germany) by trypan blue dye exclusion method. The cells were stained with 0.2% trypan blue solution and counted under a microscope using the hemocytometer.

2.4 *Cell morphological analysis*

Following QC exposure for 24 as well as 48hr, the cells were observed using an inverted optical microscope (Nikon Eclipse TS 100), and the pictures were taken using the compact digital camera attached to the microscope.

2.5 *Cytotoxicity assay*

For assessing the cytotoxic effect of QC on cells, cells were seeded at a density of 2×10^4 cells per wells in 24 well plates and were allowed to grow till the cells reached confluency. Then the cells were exposed to different concentrations of QC. Resazurin was added after an exposure period of 24 and 48hr, at a concentration of 10% to each well as per manufacturer's protocol. Readings were taken spectrophotometrically at a wavelength of 600 nm and a reference wavelength of 570 nm.

2.6 *RNA extraction and RT-PCR analysis*

Total RNA was extracted from the control and experimental cell samples as per the manufacturer's (Invitrogen, USA) protocol using TRIzol® LS Reagent. First-strand cDNA was synthesized from RNA samples (5 μg) using the cDNA synthesis kit for RT-PCR (Tetro cDNA synthesis kit) from Bioline, USA, as per specifications provided in the kit. PCR amplification of p53, Hsp70, Rac1, RhoA, Cdc45, Caspase3, Caspase8, and Caspase9 cDNA were carried out using their respective primers, designed using NCBI Primer-BLAST the online primer designing tool from NCBI site (table 1). The PCR was carried out for 30 cycles (97°C for 2 min, 94°C for 1 min, 50°C for 2 min, 70°C for 1 min). PCR products were analyzed on a 1.2% agarose gel, followed by ethidium bromide staining. The results were analyzed using a gel documentation system (BIORAD, USA).

2.7 *Acridine orange/ethidium bromide staining*

To study the different stages of apoptosis and necrosis due to QC exposure in both the cell lines, double staining was done using Acridine Orange and Ethidium Bromide. The stock concentration of 100 μg/ml of AO/EtBr was used. Cells after washing with 1XPBS and the mixed solution of AO/EtBr were added after 24 & 48 h of exposure to the drug and studied under the microscope at both 10× and 20× magnification.

2.8 *Hoechst staining*

To study the condensed pycnotic nuclei in apoptotic cells of HCT 116 & INT 407 cell line after exposure to varying concentrations of QC nuclear staining was done using Invitrogen Hoechst 33342 nucleic acid staining solution. Hoechst solution of concentration 10 mg/ml prepared. Cells were seeded in 6 well plates in the density of 5×10^4 cells/ml and exposed to the QC for 24 and 48 hr. Then plates were washed with 1XPBS; diluted Hoechst solution in 1XPBS was added in each plate, and nuclear morphology was studied using a fluorescent microscope.

2.9 *Wound healing assay*

The wound-healing assay allows studying cell motility and cell interactions. Cells were grown in 6 well plates at a seeding density of 5×10^4 cells/ml and were grown until it formed a monolayer. After a monolayer was formed a scratch was made using sterile 200 μl tips drawing a straight line from one end to another. The cells were then exposed to different concentrations of QC, and motility of the cells was studied under the microscope at 24 and 48 h time interval.

2.10 *CASPASE 3/CPP32 colorimetric assay kit*

Caspase 3 activity was determined using the CPP32 colorimetric protease assay kit (Invitrogen, Frederick,

Table 1. The names of the genes studied, reverse, and forward primer sequence with the annealing temperature

Gene of Interest		Primer set	AnnealingTemp.
18SrRNA	Forward	GTA ACC CGT TGA ACC CCA TT	50°C
	Reverse	CCA TCC AAT CGG TAG TAG CG	
Caspase 3	Forward	GCT CTG GTT TTC GGT GGG TG	65°C
	Reverse	CTG AGG TTT GCT GCA TCG AC	
Caspase 8	Forward	GAG TGA GTC ATC TCT GTT CTG CTT	65°C
	Reverse	TCA CTT CCT GTT GAG TTG ACT AGC	
Caspase 9	Forward	CTG TTC AGG CCC CAT ATG ATC G	55°C
	Reverse	AGA GCA CCG ACA TCA CCA AA	
Rac1	Forward	TCC GCA AAC AGA TGT GTT CTT A	50°C
	Reverse	GCC GAG CAC TCC AGG TAT TT	
Rho A	Forward	CCT TGT CTT GTG AAA CCT TG	60°C
	Reverse	ACT GGT AGC AAG ATG ACT TC	
Cdc42	Forward	AGA GGA AAT ACG AGG GGT GGT	65°C
	Reverse	CCT GAC TGG TCC CCA TGT TG	
P53	Forward	CCG CTC CTG GCC CCT GTC ATC TTC	50°C
	Reverse	GCA GCG CCT GAG AAC CTC CGT CAT	
HSP 70	Forward	AGC AGG CGA TAA GAT GCC AC	50°C
	Reverse	AGA CGA ATC CCT GCC GTA AA	

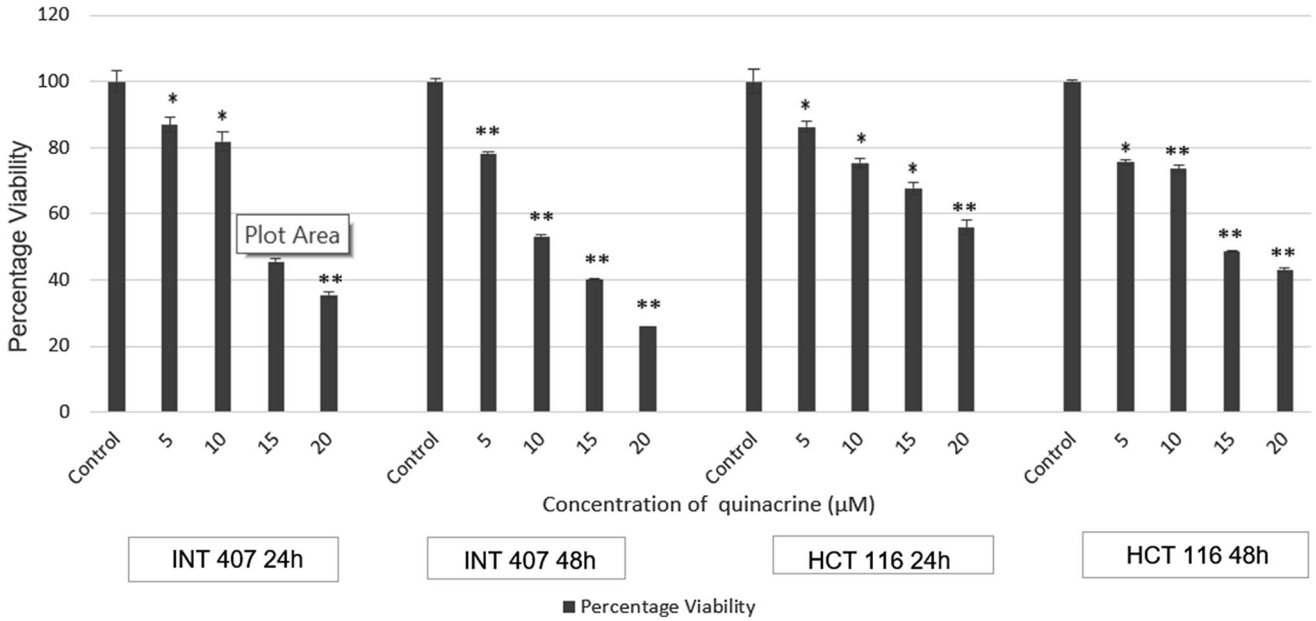

Figure 1. Cell Viability Assay of HCT 116 and INT 407 at varying concentrations of QC and exposure time. Data in the bar graphs are mean ± SE from three experiments (*p<0.05, **p<0.005).

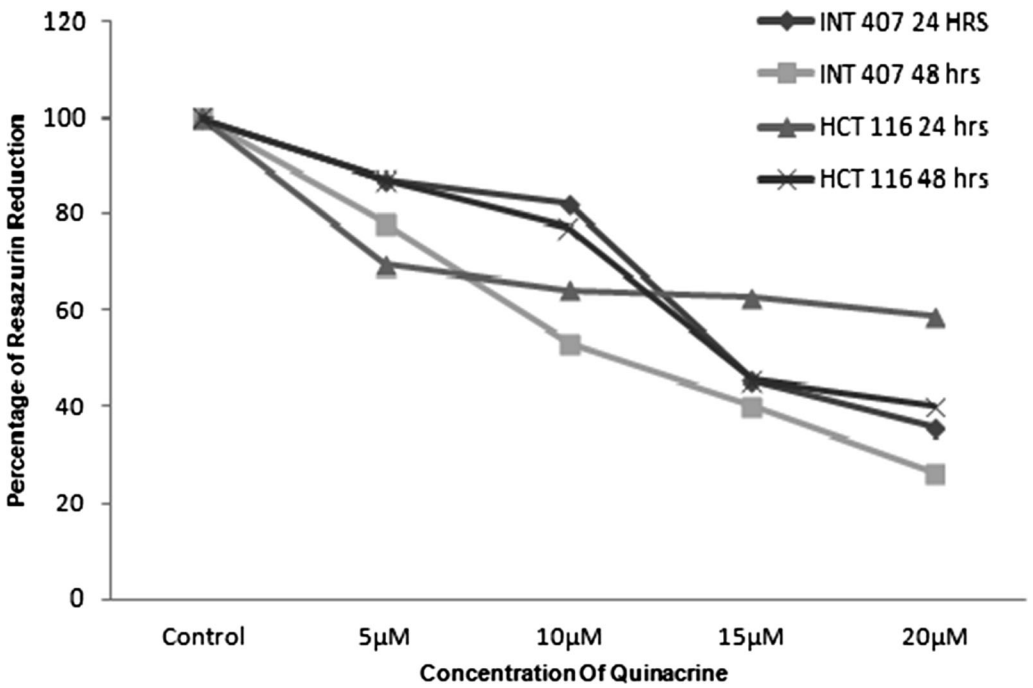

Figure 2. Resazurin Reduction Assay of HCT 116 and INT 407 at varying concentrations of QC and exposure time. Resazurin being measured at OD_{600} and Resorufin at OD_{570} is measured at doses 0 μM (positive control), 5 μM, 10 μM, 15 μM and 20 μM. The cytotoxicity is measured as a percentage reduction of resazurin compared to control. Positive control cells (without QC) are assumed to be 100% of resazurin reduction. Data in the graphs are mean ± SE from three experiments.

MD, USA) (Biovision, Life Sciences Source Catalog No. #K106). The cells were seeded at a density of 5×10^4 cells/ml in a 6 well plate and maintained at 5% CO_2 at 37°C in an incubator. Cells were treated with QC for 24 and 48 h at varying concentrations. After the treatment, cells were harvested by cell lysis buffer, and

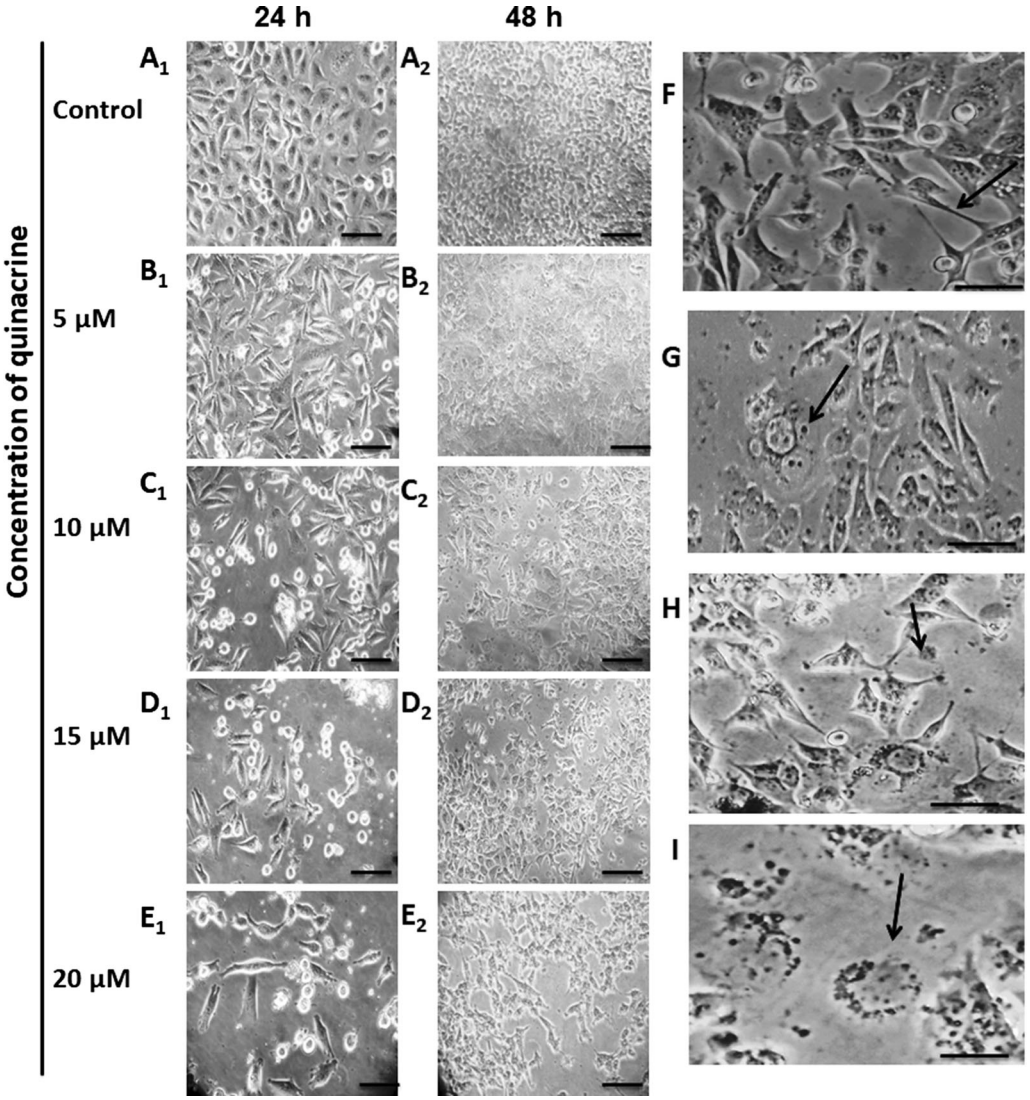

Figure 3. Cell Morphology Study of HCT 116 at varying concentrations of QC and exposure time. Inverted optical microscope (Nikon Eclipse TS 100) pictures of cells in the presence of varying concentrations of QC (200× magnification) at different exposure times. 1:24 hr, 2:48 h doses (**A_1**, **A_2**) Control, (**B_1**, **B_2**) 5 µM, (**C_1**, **C_2**) 10 µM, (**D_1**, **D_2**) 15 µM and (**E_1**, **E_2**) 20 µM (Scale Bar 40 µm). Localized pictures of varying morphological changes in cells-24 h of (**F**) 15 µM, (**G**) 20 µM and 48 h of (**H**) 15 µM, (**I**) 20 µM (Scale Bar 20 µm).

200 µg of protein lysate each was loaded into a 96 well plate. Caspase 3 activity was determined by adding DEVD-pNA substrate followed by incubation for 2 h in the dark at 37°C (as per the kit). The absorbance was measured at 405 nm using an ELISA microplate reader.

2.11 *Data analysis*

All experiments were done in triplicates to get comparative data. Student T-test and the standard deviation were calculated to get the significant values and differences between each set of experiments. Results were expressed as the Standard Error Mean (SEM) of data obtained from three independent experiments. P-value 0.05 was considered statistically significant for all tests.

3. Results

3.1 *Effect of QC on cell viability*

Trypan blue dye exclusion method was used to determine the cell viability of HCT 116 and INT 407 cell lines on exposure to a different concentrations of QC. The graph shows the percentage viability against the different concentrations of QC. A dose-dependent

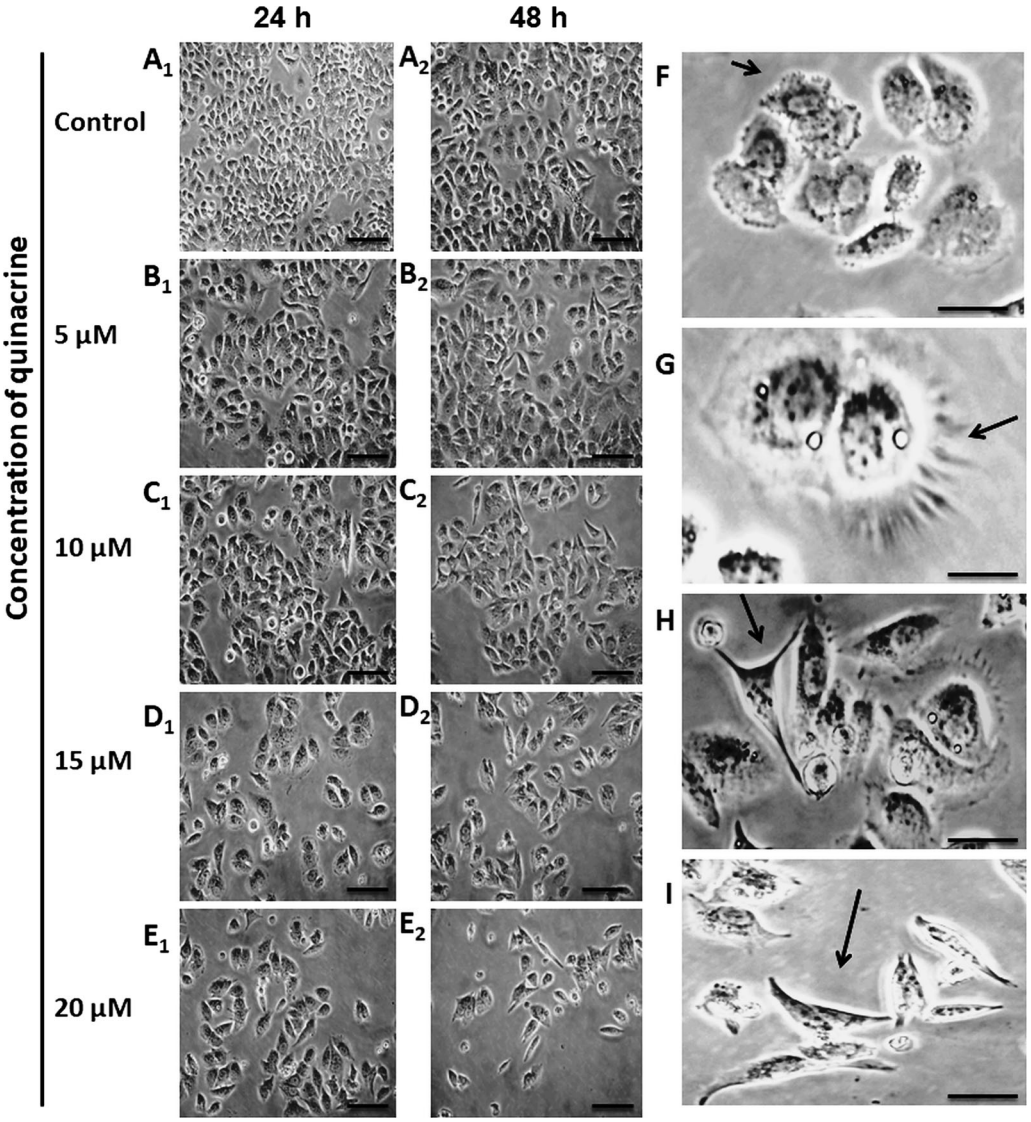

Figure 4. Cell Morphology Study of INT 407 at varying concentrations of QC and exposure time. Inverted optical microscope (Nikon Eclipse TS 100) pictures of cells in the presence of varying concentrations of QC (200× magnification) at different exposure times. 1:24 hr, 2:48 h dose (**A_1**, **A_2**) Control, (**B_1**, **B_2**) 5 µM, (**C_1**, **C_2**) 10 µM, (**D_1**, **D_2**) 15 µM and (**E_1**, **E_2**) 20 µM (Scale Bar 40 µm). Localized pictures of varying morphological changes in cells-24 h of (**F**) 15 µM, (**G**) 20 µM and 48 h of (**H**) 15 µM, (**I**) 20 µM (Scale Bar 20 µm).

cytotoxicity was observed in both cancer cell lines when compared to its control. INT 407 cells exposed to QC showed percentage viability of 86%, 81%, 45% and 35% for respective doses of 5 µM, 10 µM, 15 µM and 20 µM at 24 hr. At 48 h the percentage reduced to 78%, 53%, 40% and 26% when incubated with QC. A similar pattern of cell viability was observed in the HCT 116 cell line when exposed to varying concentrations of QC. At 24 h of incubation, the viability percentage was 86%, 75%, 67%, and 55% at 5 µM, 10 µM, 15 µM and 20 µM at 24 h of QC exposure. There was a further reduction in the percentage of viable cells when incubated for 48 h timepoint showing 75%, 73%, 48% and 43% at 5 µM, 10 µM, 15 µM and 20 µM of QC.

3.2 *Metabolic activity by resazurin reduction assay*

The reduction in metabolic activity of the two cell lines due to QC exposure was studied by resazurin reduction assay. Our findings suggest that there was a decrease in cell metabolic activity with the increase in the concentration of QC (figure 2), which is comparable to the conclusions of the trypan blue dye

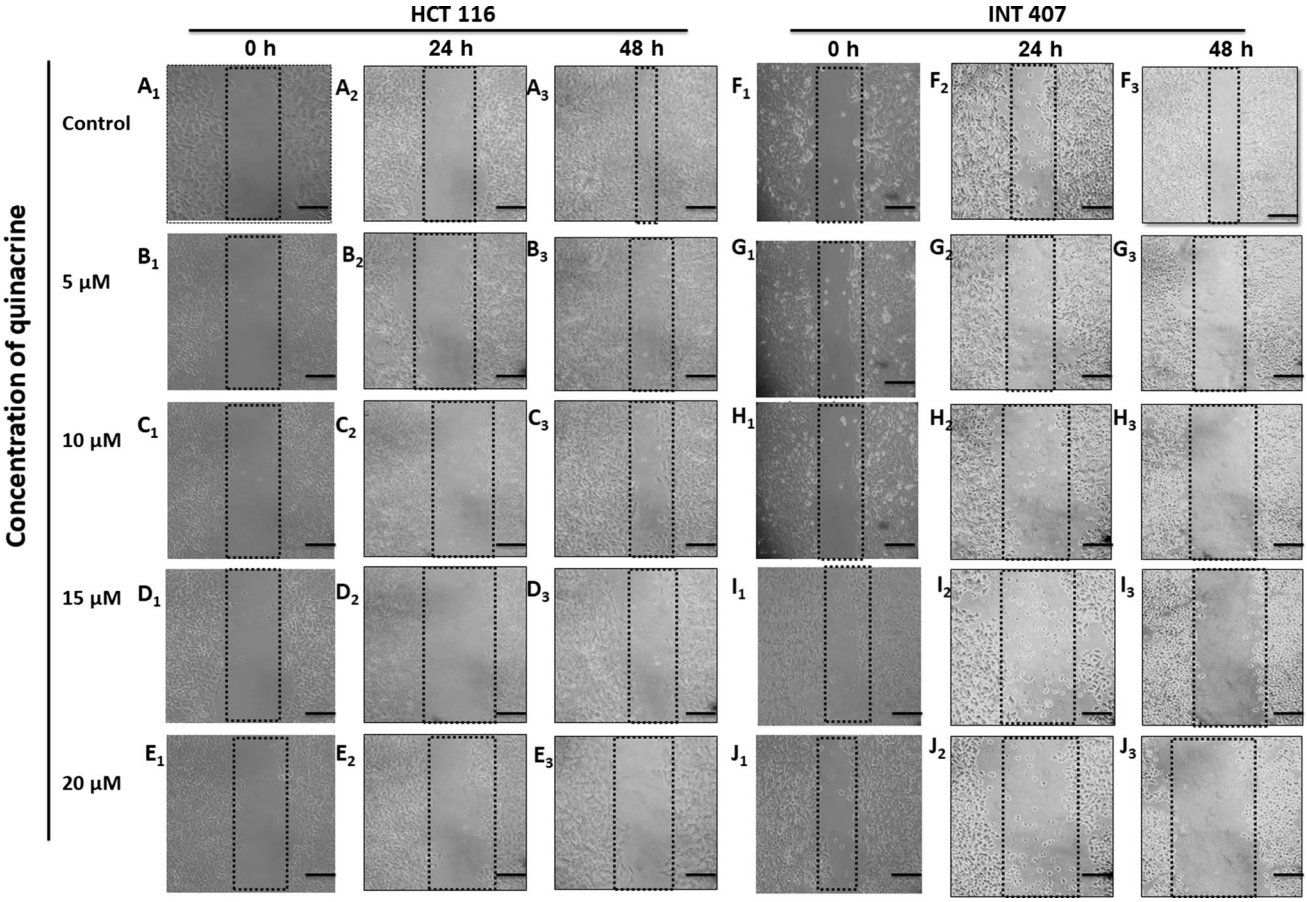

Figure 5. Wound closure activity of treated HCT 116 and INT 407 cells after 24 and 48 h at varying concentrations of QC. Representative photographs of wounded cell monolayer treated with QC. The typical result from three independent experiments is shown (Scale Bar 40 µm).

exclusion method (figure 1). The percentage of death reduced from 31% at 24 h and 27% at 48 h in INT 407 cell line. Further, it was observed that the reduction in cell viability was 54% for 24 h and 33% at 48 h for HCT 116 (figure 2) cell line at 20 µM of QC. Even though the cytotoxicity increased in both cell lines, there was a significant difference in their IC_{50} values. It was 8.18 µM for INT 407 and 5.14 µM in HCT 116 cell lines.

3.3 *Morphological analysis of QC exposure*

QC had a time and dose-dependent effect on both the cell lines HCT 116 (figure 3A–E) and INT 407 (figure 4A–E). At higher concentrations (15 and 20 µM) in both the cell lines (figures 3E_1, E_2, and 4E_1, E_2), a microscopic study reveals that the cell was not attached to the surface and was rounded off. There was a loss in a cell to cell contact; even different morphological distributions could be seen in HCT 116 and INT 407 cell lines (figures 3G, H, and 4G, H) upon exposure to QC. In HCT 116, the formation of filopodia and lamellipodial structures were seen in figure 3F (15 µM) and 3G (20 µM) at 24 h. The cells seemed to be ruptured at the same concentration (figure 3H showing 15 µM concentration of QC and figure 3I showing 20 µM of QC at 48 h). INT 407 at higher concentration revealed filopodia structures (figure 4F–G) 4F being the 15 µM and 4G being the 20 µM of 24 h upon exposing with QC and at 48 h time point showed elongated structure (figure 4H–I, exposed to 15 µM and 20 µM of QC), suggesting QC modulating cell cytoskeleton.

3.4 *Effect of QC on cellular motility*

In the wound healing assay, both HCT 116 control cells showed complete wound closure activity in 48 h. In

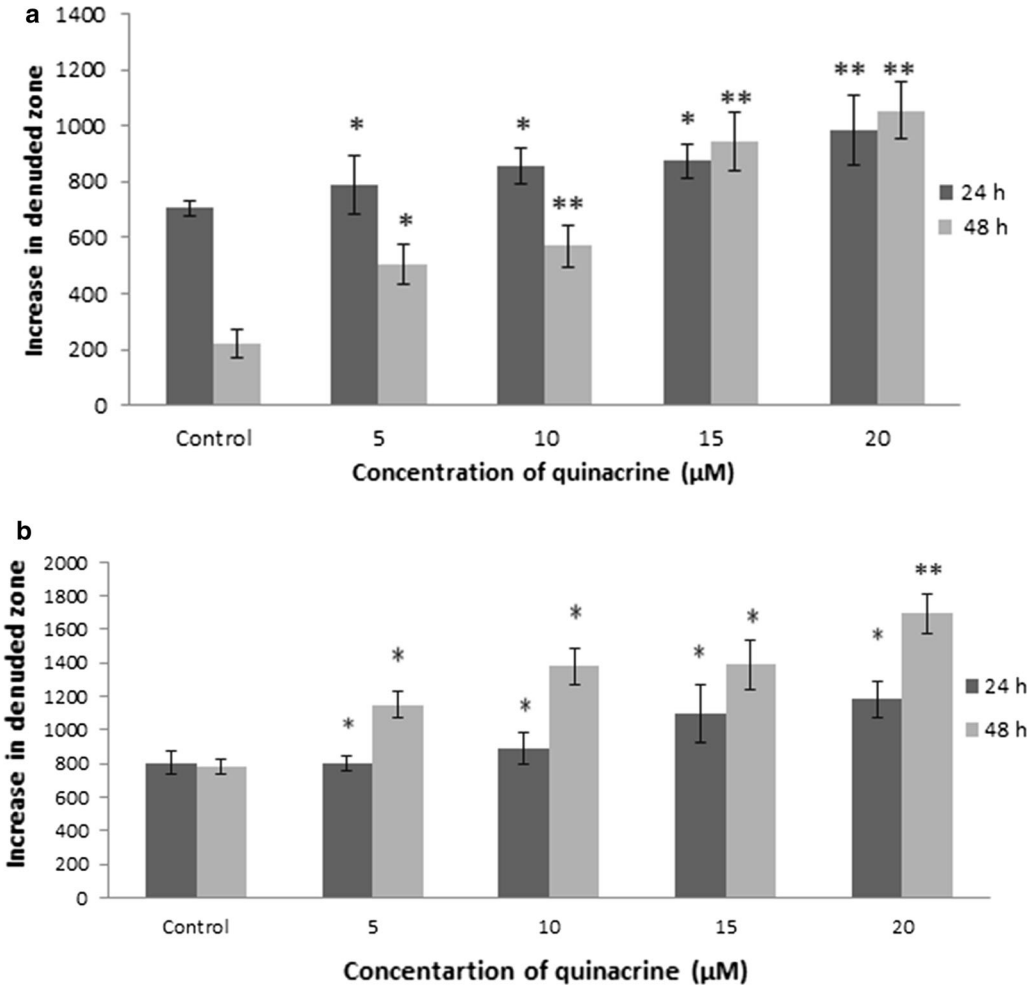

Figure 6. Quantitative assessment of motility inhibition rate of QC on (**a**) HCT 116 and (**b**) INT 407 cell lines. Treatment with QC reduced the migratory effect of both the cell lines (**a**) HCT 116 (**b**) INT 407, and the distance in the denuded zone increased time and exposure dependently. Data in the bar graphs are mean ± SE from three experiments (*$p<0.05$, **$p<0.005$).

INT 407 cells at 24 and 48 h of control cells showed a reduction in a denuded zone as compared to T0 h (figure 5A_1–J_1). With varying concentrations of QC at a different time point (figure 5A_1–J_3) showed a drastic reduction in wound closure activity after 24 and 48 h of both the cell line HCT 116 and INT 407. At the end of the different incubation periods, the treated cells showed a limited wound closure activity (figures 5E_1–E_3, 5J_1–J_3, and 6A–B). An increase in distance of the denuded zone was both time and dose-dependent. Even at the lowest concentration of QC, inhibition of motility was seen as 20% in HCT 116 and 30% in INT 407 cell line (figures 5 and 6A–B). In the study, it was observed that the motility property was hindered for both the cell lines with time and varying concentrations of QC. In INT 407, the gap increased from 750 to 1600 when exposed to 20 µM of QC as compared to that in HCT 116, the denuded zone increased from 200 to 1100.

3.5 *Fluorescence microscopic analysis of cell death induced by QC*

We used two different fluorescent assays.

3.5.1 *Acridine orange/ethidium bromide staining:* In Ao/EtBr stain there can be three possibilities (i) Viable cells would have uniform nuclei showing green fluorescence with organized structure, (ii) early apoptosis would have intact membrane showing the beginning of DNA cleavage and exhibit green patches or fragments, (iii) cells undergoing late apoptosis would fluorescence orange to red with condensed chromatin. After 24 and 48 h of QC exposure to HCT 116 (figure 7A_1–E_1 and A_2–E_2), cells appeared to exhibit fragmented nuclei and condensed chromatins emitting orange to red fluorescence when stained under higher concentrations of QC (figure 7D_1 and E_1). Comparatively, in 48 h, we could observe cells in

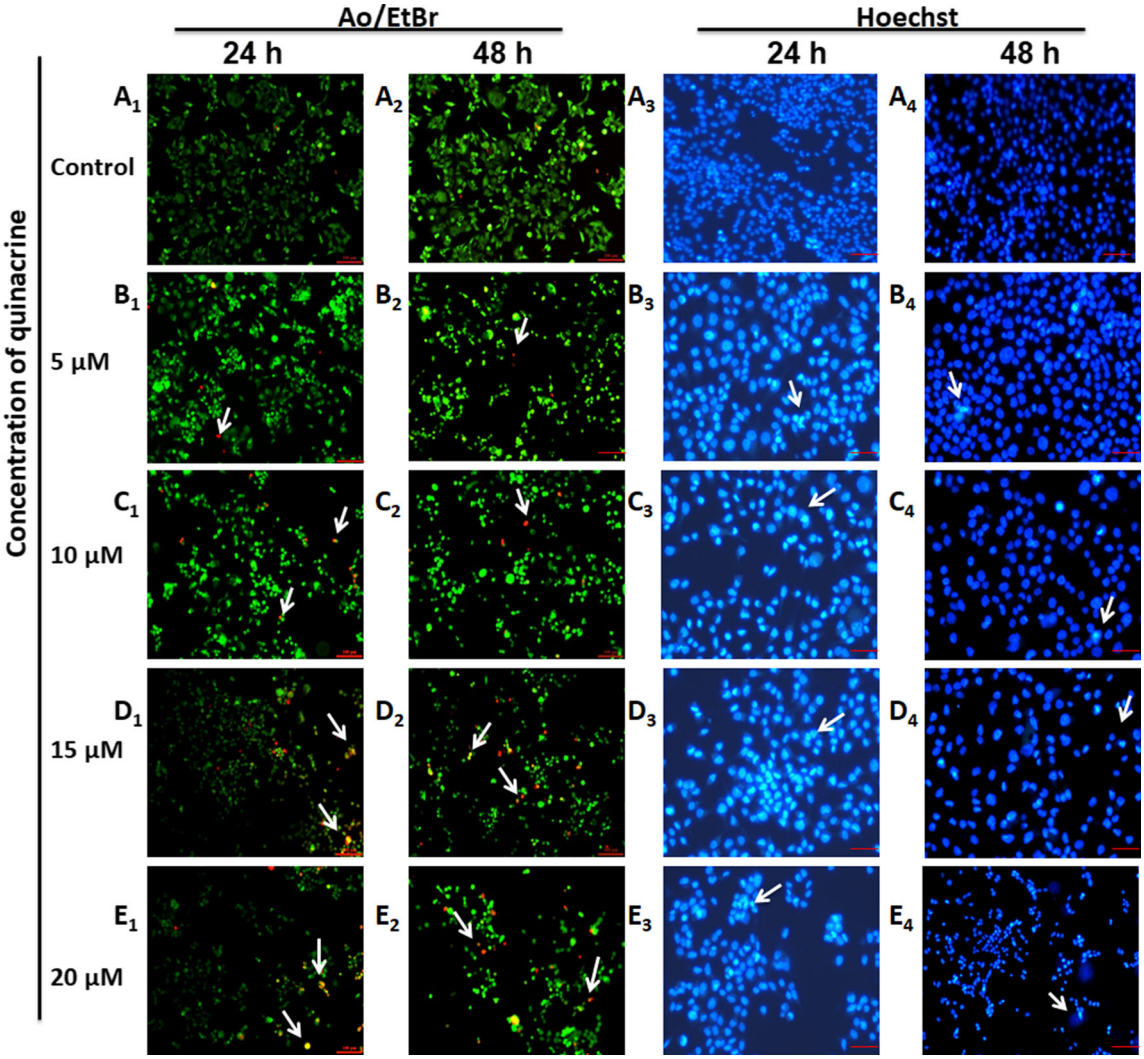

Figure 7. Images of HCT 116 stained with Ao/EtBr (panel 1) and Hoechst 33342 (panel 2) after exposure to varying concentrations of QC and time points. In Panel 1, cells are stained with Ao/EtBr. (**A_1–A_2**) Viable cells were having uniform green nuclei, (**B_1–E_2**) Early apoptotic cells with green patches showing condensed DNA and orange to red color pointing late apoptotic cells. The red to orange color showing condensed and fragmented DNA increased in number with exposure time and concentration of QC as compared to its positive control. In Panel 2 (**A_3–A_4**), cells stained with Hoechst nuclear appeared round and evenly stained since untreated. In (**B_3–E_4**) cells are treated, and the number of intensely stained cell numbers increased with concentration and time. These intense stains are fragmentized and condensed DNA leading to or in apoptosis. At the highest concentration e_4, there is rarely any cell having round and evenly stained (Scale Bar 40 µm).

early or late apoptosis (figure 7E_2). In INT 407 cell line both in 24 and 48 h (figure 8A_1–E_1 and A_2–E_2), apoptotic cells with orange to red fluorescence, which increased with the concentration of QC (figure 8E_1 and E_2). Apoptotic cells were counted after exposure to varying concentrations of QC for both the cell lines.

It was observed that after exposures to QC, the cells were undergoing apoptosis in both the cell lines as compared to their respective controls (figure 9).

3.5.2 *Hoechst staining:* Hoechst is widely known for detecting cells undergoing apoptosis and nuclear fragmentation. To analyze the process of cell death, cells were exposed to QC and studied at 24 and 48 h time-point. In the HCT 116 cell line, the fragmented DNA was documented at 10 µM onwards at 24 h time-point (figure 7A_3–E_3) and at 48 h very fewer cells being attached showed a high number of apoptotic cells at the highest concentration of QC (figure 7E_3).

It was observed in both the cell lines that the number of apoptotic nuclei increased with the increase in concentration of QC under both staining procedures. But HCT 116 was seen as having higher apoptotic nuclei as compared to INT 407 cell line except at 20 µM of QC

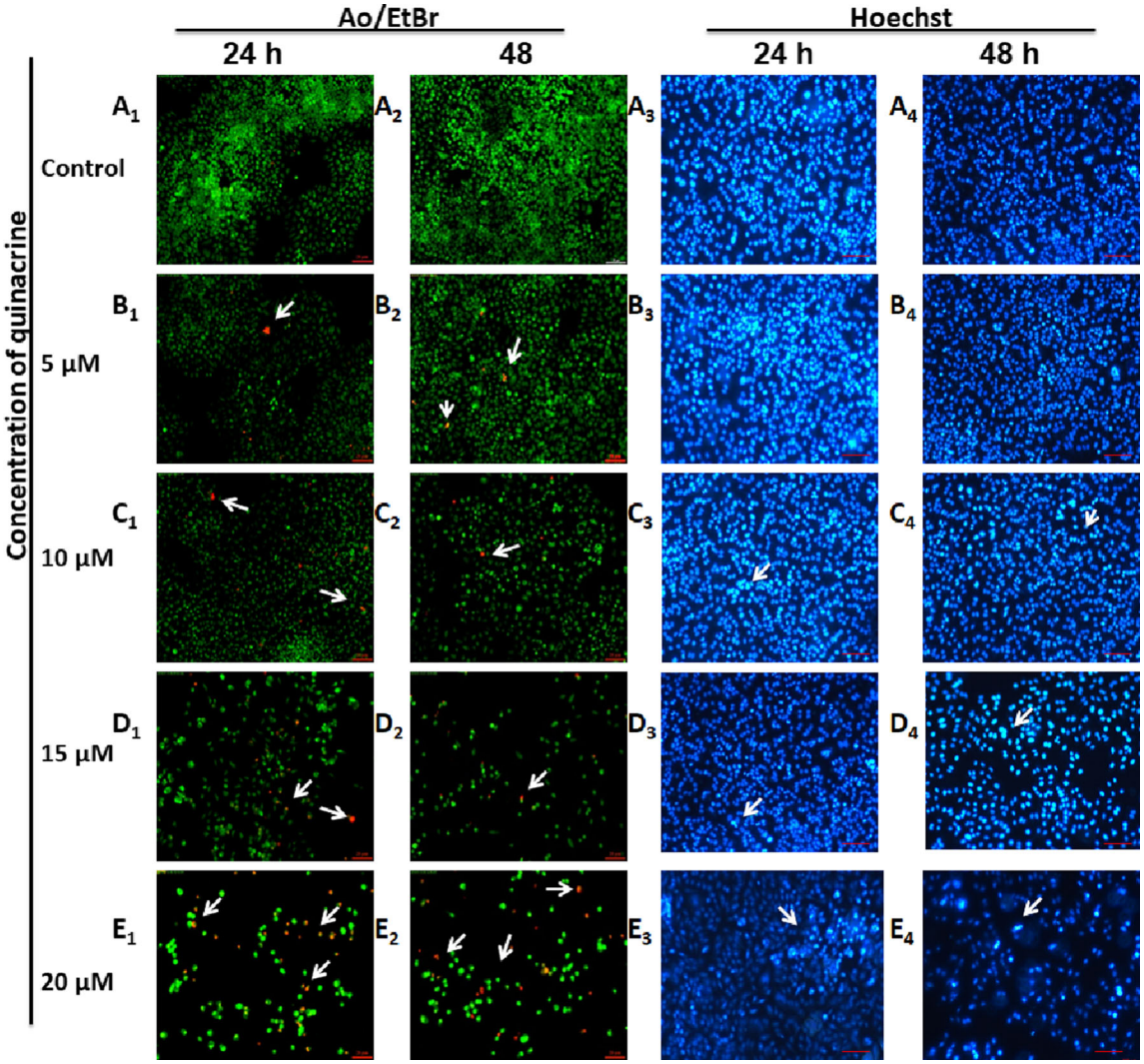

Figure 8. Images of HCT 116 stained with Ao/EtBr (panel 1) and Hoechst 33342 (panel 2) after exposure to varying concentrations of QC and time points. In Panel 1, cells are stained with Ao/EtBr. ($\mathbf{A_1}$–$\mathbf{A_2}$) Viable cells are having uniform green nuclei, ($\mathbf{B_1}$–$\mathbf{E_2}$) Early apoptotic cells with green patches showing condensed DNA and orange to red color pointing late apoptotic cells. The red to orange color showing condensed and fragmented DNA increased in number with exposure time and concentration of QC as compared to its positive control. In Panel 2 ($\mathbf{A_3}$–$\mathbf{A_4}$), cells stained with Hoechst nuclear appeared round and evenly stained since untreated. In ($\mathbf{B_3}$–$\mathbf{E_4}$) cells are treated, and the number of intensely stained cell numbers increased with concentration and time. These intense stains are fragmentized and condensed DNA leading to apoptosis (Scale Bar 40 µm).

both for 24 & 48 h (figure 9). In HCT 116 at the highest concentration, very few cells were attached; the apoptotic INT 407 cells outnumbered HCT 116 cells.

3.6 *Activation of ICE-family proteases/caspases by QC leading to apoptosis*

Though there was not a much significant difference in 24 h of HCT 116 at 48 h as compared to that in control, the 20 µM of QC exposure showed three-fold increase in the expression of caspase 3 activity. In INT 407 cell line both for 24 and 48 h, the caspase 3 activity is 2.5- and 3-fold, respectively (figure 10). It can be implied from the data that as the concentration of QC increased, the caspase 3 in the translational level is also increasing of cells towards apoptosis.

3.7 *QC induced expression profile of small GTPases and apoptotic genes at their mRNA level*

3.7.1 *mRNA level expression of small GTPases:* It was seen for 24 and 48 h the mRNA expression of Rac1

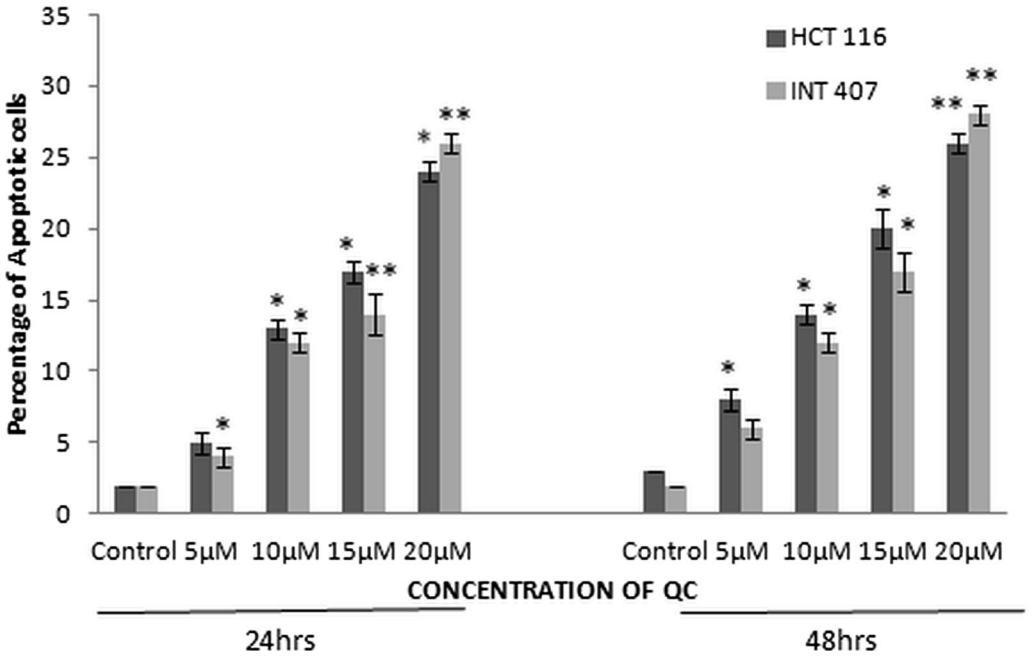

Figure 9. Apoptotic index by AO/EB staining of HCT 116 and INT 407 cells treated with different concentrations of QC for 24 h and 48 hr. Data in the bar graphs are mean ± SE from three experiments (*p<0.05, **p<0.005).

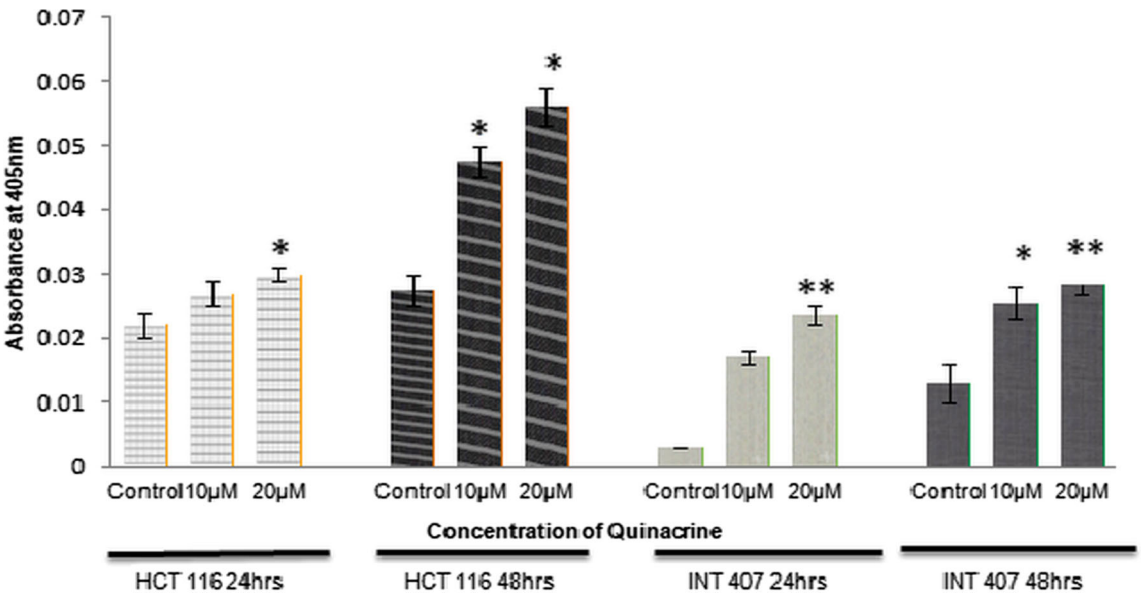

Figure 10. Activation of caspase 3 in HCT 116 and INT 407 at varying concentrations of QC and exposure time. Cells were treated with varying concentrations of QC, and then whole-cell protein was extracted and processed according to caspase 3/CPP32 Colorimetric Assay Kit. Data in the bar graphs are mean ± SE from three readings at 405 nm (*p<0.05, **p<0.005).

and Cdc42 was quite high, which was both time and concentration-dependent (figures 11 and 17a) in the HCT 116 cell line. In Rac1, the expression increased from 0.4 to 0.6 and in Rho A from 1 to 0.2. mRNA level expression of RhoA started going down from 5 μM onwards from 1 to 0.2 at 24 h (figure 17A). In INT 407, we have not seen any drastic change in the expression pattern of small GTPases at the mRNA level at 24 h and 48 h (figures 12 and 17A). In Rac1, the expression changes from 0.6 to 0.7, RhoA from 2 to 3, and CDC42 from 1.6 to 3. In 48 h any drastic change was not documented in any of the cell lines.

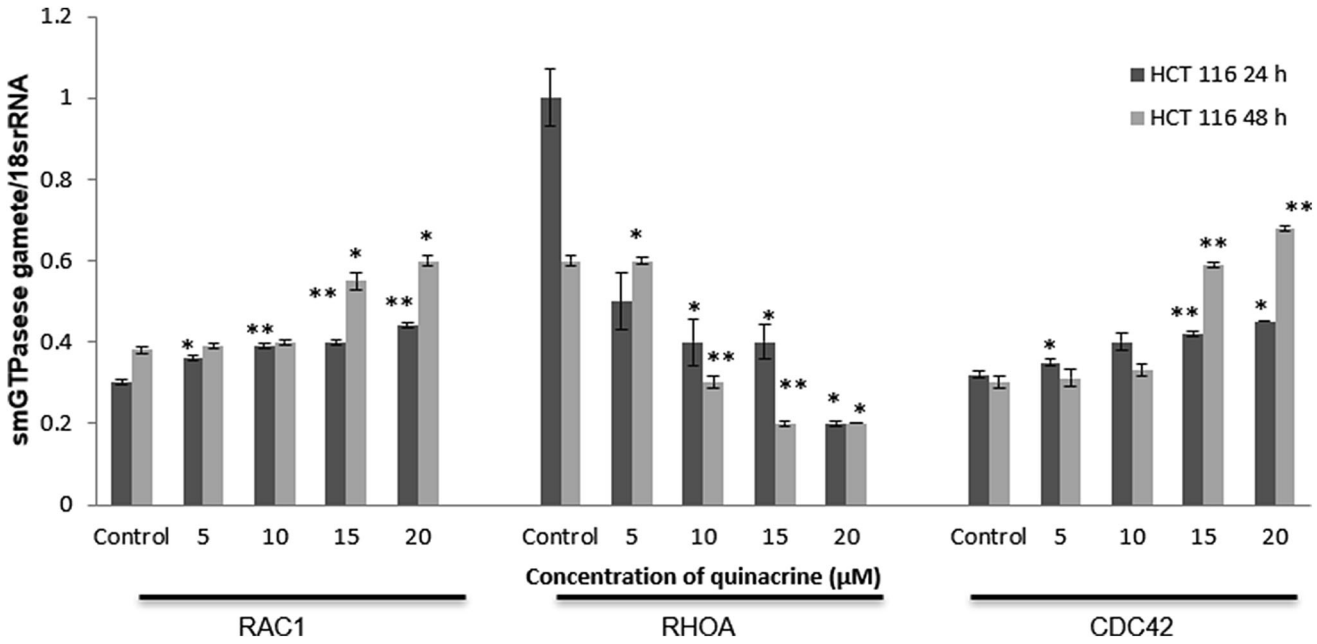

Figure 11. RT-PCR relative gene expression of Small GTPases levels of HCT 116 at 24 h and 48 h time point with exposure to different varying concentrations of QC. The results of the quantitative RT-PCR validation experiments are shown in the graph. The bars depicted are in folds change in expression of small GTPases relative to 18srRNA. Data in the bar graphs are mean ± SE from three experiments (*$p<0.05$, **$p<0.005$).

3.7.2 *Hsp70 expression analysis:* It was observed that in both the cell lines with time and concentration, there was an increase in the HSP 70 expression at the mRNA level. In HCT 116, the expression pattern of HSP 70 at transcriptional level showed an increase in expression about three folds for 48hr, as compared to that in control. In INT 407 for 24 h, the expression remained constant after 10 μM (figures 13 and 17B).

3.7.3 *P53 expression analysis:* p53 mRNA expression showed 2-folds and 4-folds increase in expression pattern for HCT 116 cell line for 24 and 48 h. In contrast, INT 407 cell line did not show much difference in the expression pattern of p53 at the mRNA level with incubation time and varying exposure (figures 14 and 17B).

3.7.4 *Caspase cascade expression profile pertaining to apoptosis:* Caspase 8 being initiator caspases and caspase 3 as executioner caspase were studied after the exposure to a different concentration of QC. It was observed that in both the cell lines, QC induced the expression of both the caspase 3 and 8 in time and dose-dependent manner. In HCT 116, caspase 3 is induced by 2-folds, whereas, in INT 407, it is increased marginally (figures 15, 16 and 17C). Caspase 8 showed an increased expression pattern in both the cell lines like executioner caspase 3 (figures 15 and 16). Caspase 9 showed a decreased expression pattern at the mRNA level in 2-fold and 2.5-fold for HCT 116 in 24 and 48 h exposure to QC (figures 15 and 16). INT 407 cell line showed a decreased expression pattern, but it was not as significant as compared to that in the HCT 116 cell line.

4. Discussion

Colon cancer is mediated by the transformation of colonic epithelial cells into colon adenocarcinoma cells. This process of change involves gradual mutations of the *Adenomatous Polyposis Coli* (APC) gene followed by KRAS, PIK3CA, transforming growth factor-β, and p53 gene mutations (Grady and Carethers 2008; Preet *et al.* 2012). Two predominant forms of genomic instability in colon cancers were identified as microsatellite instability and chromosome instability (Pancione *et al.* 2012; Tahir *et al.* 2015). A peptic ulcer is a common disorder that is multifactorial, and the treatment faces great difficulties. This disorder is usually observed in the stomach and proximal duodenum (Maity *et al.* 2003). In this context, it will be fascinating to study the drug effect of a medicinal plant source or a natural product.

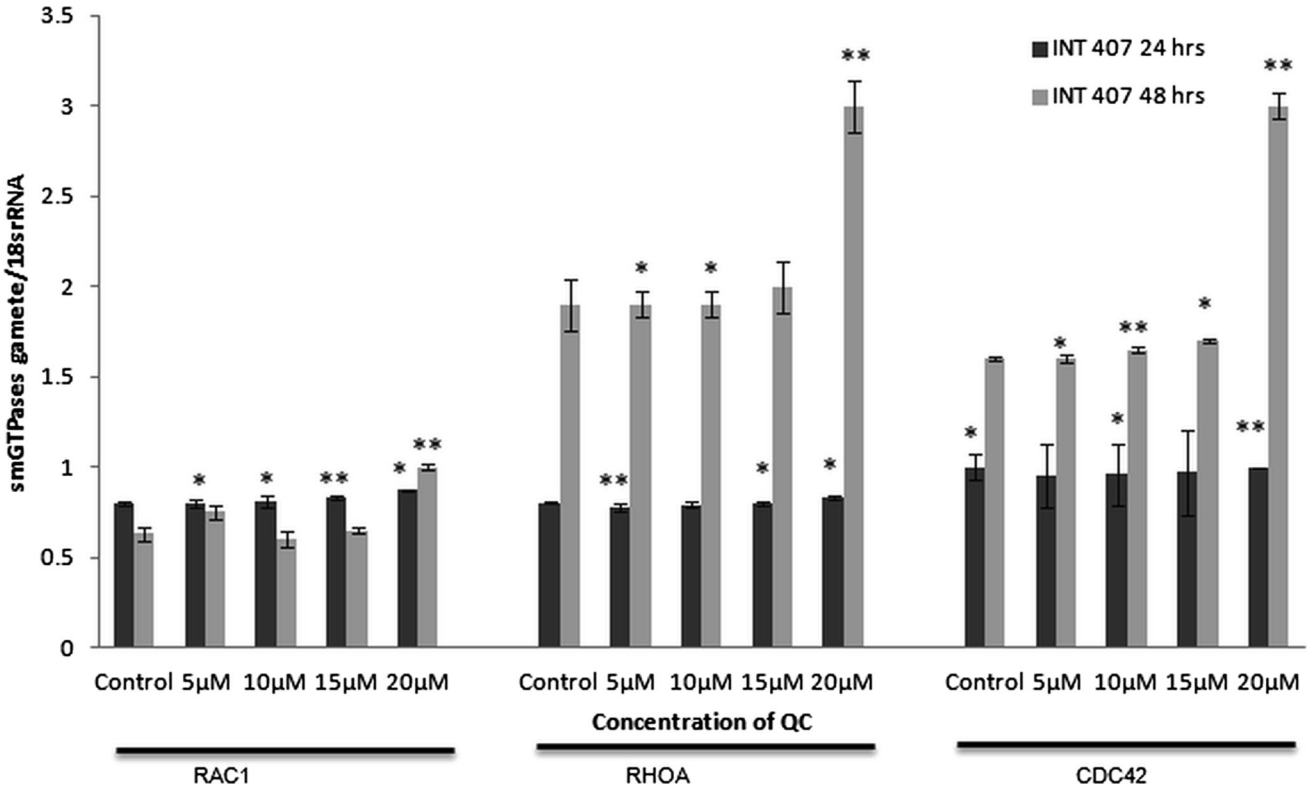

Figure 12. RT-PCR relative gene expression of Small GTPases levels of INT 407 at 24 h and 48 h time point with exposure to different varying concentrations of QC. The results of the quantitative RT-PCR validation experiments are shown in the graph. The bars depicted are in folds change in expression of small GTPases relative to 18srRNA. Data in the bar graphs are mean ± SE from three experiments (*p<0.05, **p<0.005).

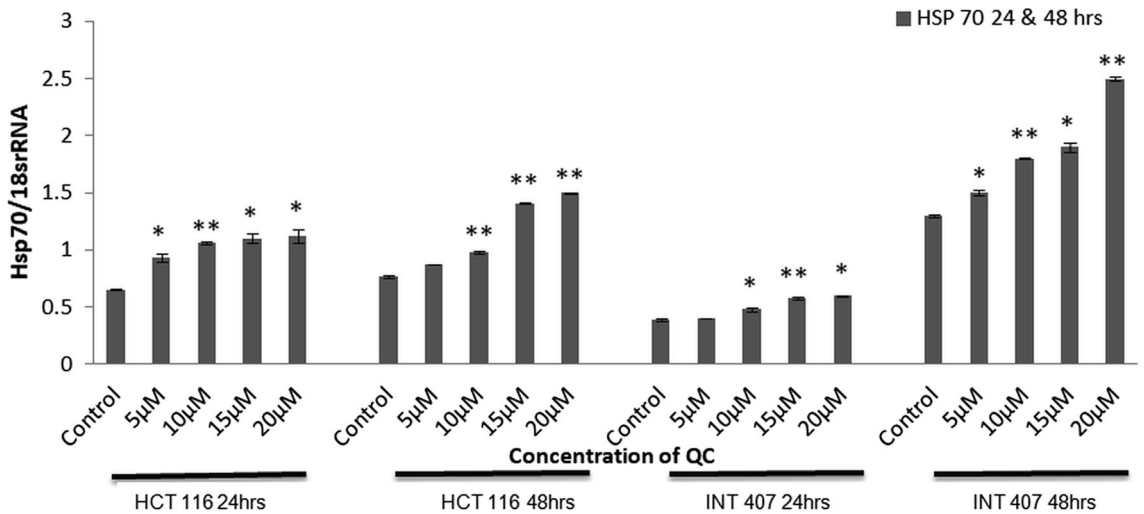

Figure 13. RT-PCR relative gene expression of HSP 70 of HCT 116 and INT 407 at 24 h and 48 h time point with exposure to different varying concentrations of QC. The results of the quantitative RT-PCR validation experiments are shown in the graph. The bars depicted are in folds change in expression of small GTPases relative to 18srRNA. Data in the bar graphs are mean ± SE from three experiments (*p<0.05, **p<0.005).

Many studies have been completed using natural products and constituting phytochemical compounds, which are potential chemopreventive agents (Gurova *et al.* 2005). Recently, it has been shown that QC a derivative of 9-aminoacridine, which was discovered in 1920 for different kinds of diseases possess anticancer

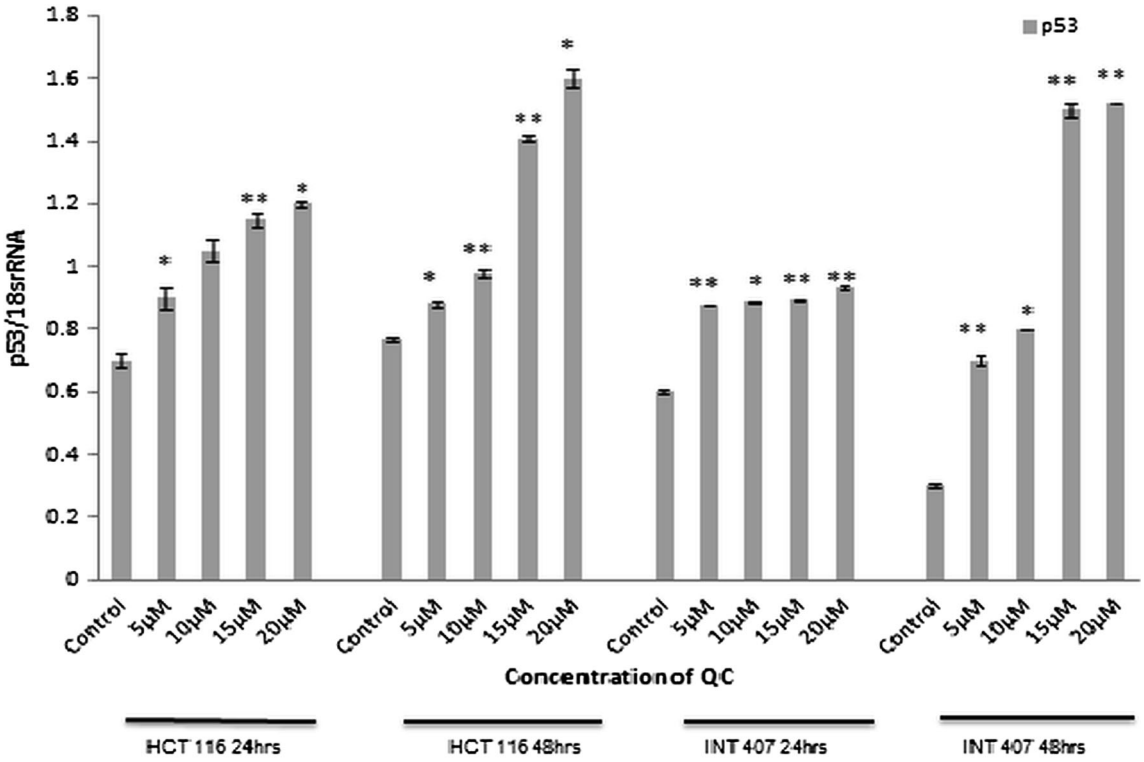

Figure 14. RT-PCR relative gene expression of p53 of HCT 116 and INT 407 at 24 h and 48 h time point with exposure to different varying concentrations of QC. The results of the quantitative RT-PCR validation experiments are shown in the graph. The bars depicted are in folds change in expression of p53 relative to 18srRNA. Data in the bar graphs are mean ± SE from three experiments (*$p<0.05$, **$p<0.005$).

activities in pancreatic and renal cell carcinoma (Upcroft and Upcroft 2001; Gupta *et al.* 2003; Moghaddam *et al.* 2005; Goodell et al. 2008; Gurova 2009; Lalitha *et al.* 2016). In this study, we have investigated the anticancer activity of QC in cancer cell lines. We have shown the time and dose-dependent effect of QC on cellular morphology alteration, including expression and regulation pattern of GTPases and caspase cascade at the transcriptional level of colorectal cancer and gastric ulcer cell line.

In the present study, we have evaluated the anti-cancer potential of QC on HCT 116 and INT 407 cell lines by studying its effect on apoptosis induction, motility, and crucial genes regulating cytoskeleton modulation like Rac1, RhoA and Cdc42 at mRNA level. Analysis of cell count by trypan blue dye exclusion method and resazurin reduction assay depicts a significant amount of cell death, which was time and dose-dependent (Celisa Santimano *et al.* 2013). Cell motility was found to be reduced which may be correlated with the cytotoxic effect of QC. The cell motility assay indicates that QC could stop the motility of cancer cells (Jeong *et al.* 2011). A significant decrease in motility was also observed around concentration near to IC_{50} concentration, and at lower concentrations, motility was suppressed (Hall 2009). Progression of cancer is characterized by features of invasiveness, which includes defects in cellular morphogenesis that lead to tissue disruption, acquisition of migratory and invasive characteristics, and also the generation of genomic instability through defects in the mitosis other than usual features. With relevance to cancer, it was observed that the cytoskeleton plays a crucial role in the progression of cancer in (i) cell cycle, (ii) morphogenesis, and (iii) migration (Hall 2009). In our study, we observed in the denuded zone, different kinds of cytoskeleton modulations such as lamellipodial protrusions and the formation of filopodial structures, which led to the expression of Rac1, RhoA, and Cdc42 was documented. Our study throws light on the activation of Rac1 and Cdc42 upon QC exposure to show that there was a decrease in the expression of RhoA at the basal level when compared to its control in HCT 116. However, in INT 407 cell line, the denuded zone exhibited various modulations, and activation of all the three genes. It is concluded from the study that QC was able to down-regulate master gene for cell cytoskeleton modulation which is RhoA since RhoA

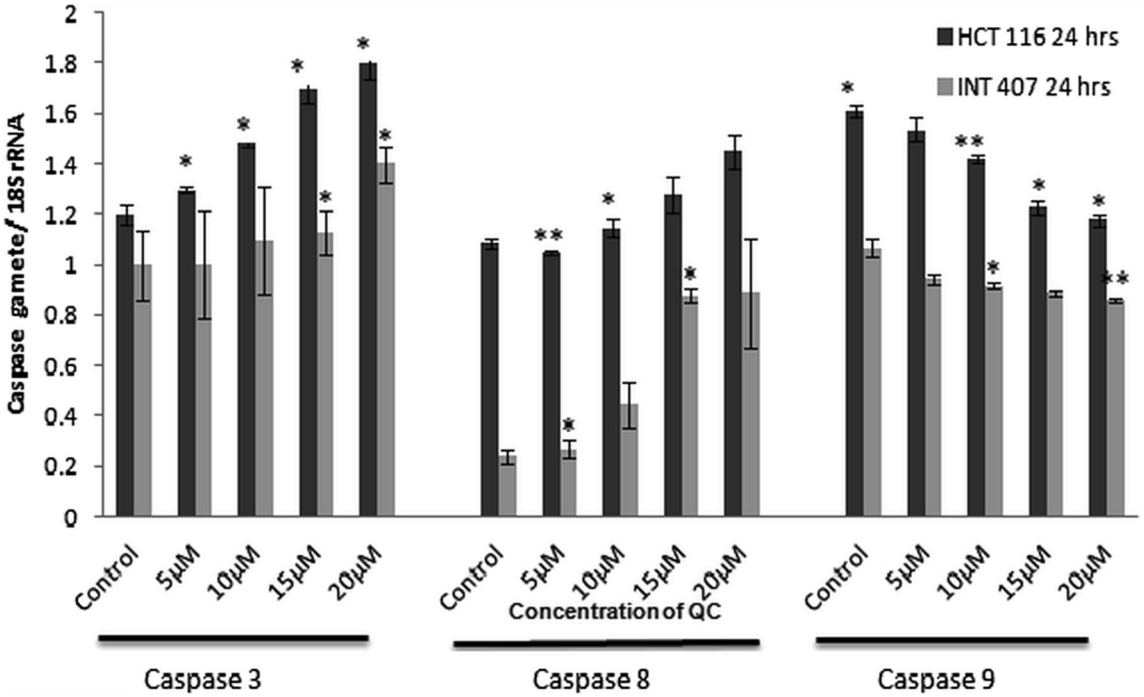

Figure 15. RT-PCR relative gene expression of caspase cascade in HCT 116 and INT 407 at a 24 h time point with exposure to different varying concentrations of QC. The results of the quantitative RT-PCR validation experiments are shown in the graph. The bars depicted are in folds change in expression of caspase 3, 8 & 9 relative to 18srRNA. Data in the bar graphs are mean ± SE from three experiments (*p<0.05, **p<0.005).

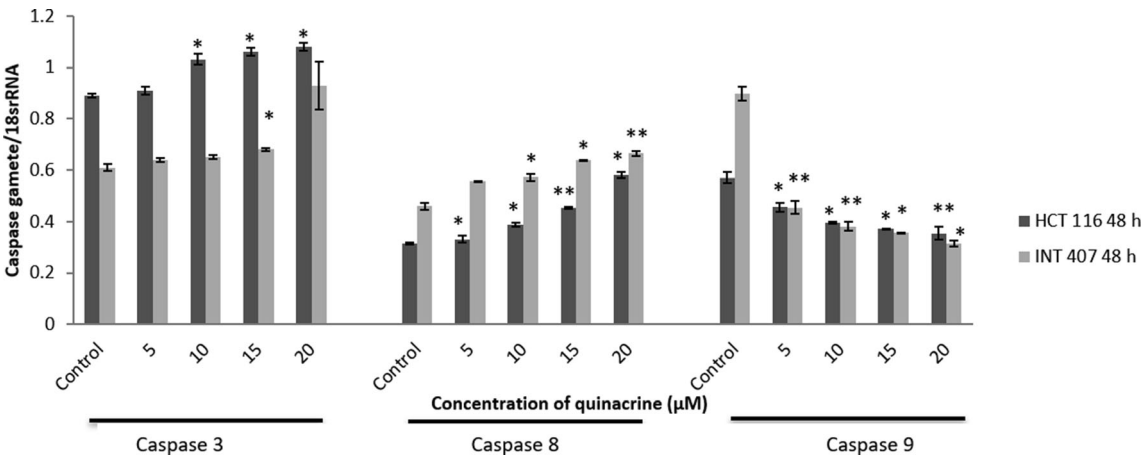

Figure 16. RT-PCR relative gene expression of caspase cascade in HCT 116 and INT 407 at 48 h time point with exposure to different varying concentrations of QC. The results of the quantitative RT-PCR validation experiments are shown in the graph. The bars depicted are in folds change in expression of caspase 3, 8 & 9 relative to 18srRNA. Data in the bar graphs are mean ± SE from three experiments (*p<0.05, **p<0.005).

plays a role in tumor cell proliferation, cell survival and in stimulating transformation. During motility it was observed by previous workers that Rac activation at the front and Rho activation at the rear promote migration (Hall 2009; Pertz *et al.* 2006). The lack of migrating capability with QC concentration might be attributed to the down-regulation of RhoA as well.

Apoptosis of cells involves a series of events with the onset of the release of cytochrome C from mitochondria, activation of a series of caspases and eventually fragmentation of DNA (Harikumar *et al.* 2009). Caspase 3 is expressed in both the pathways irrespective of its being intrinsic or extrinsic since it is an 'executioner' caspase. Caspase 8 and caspase 9

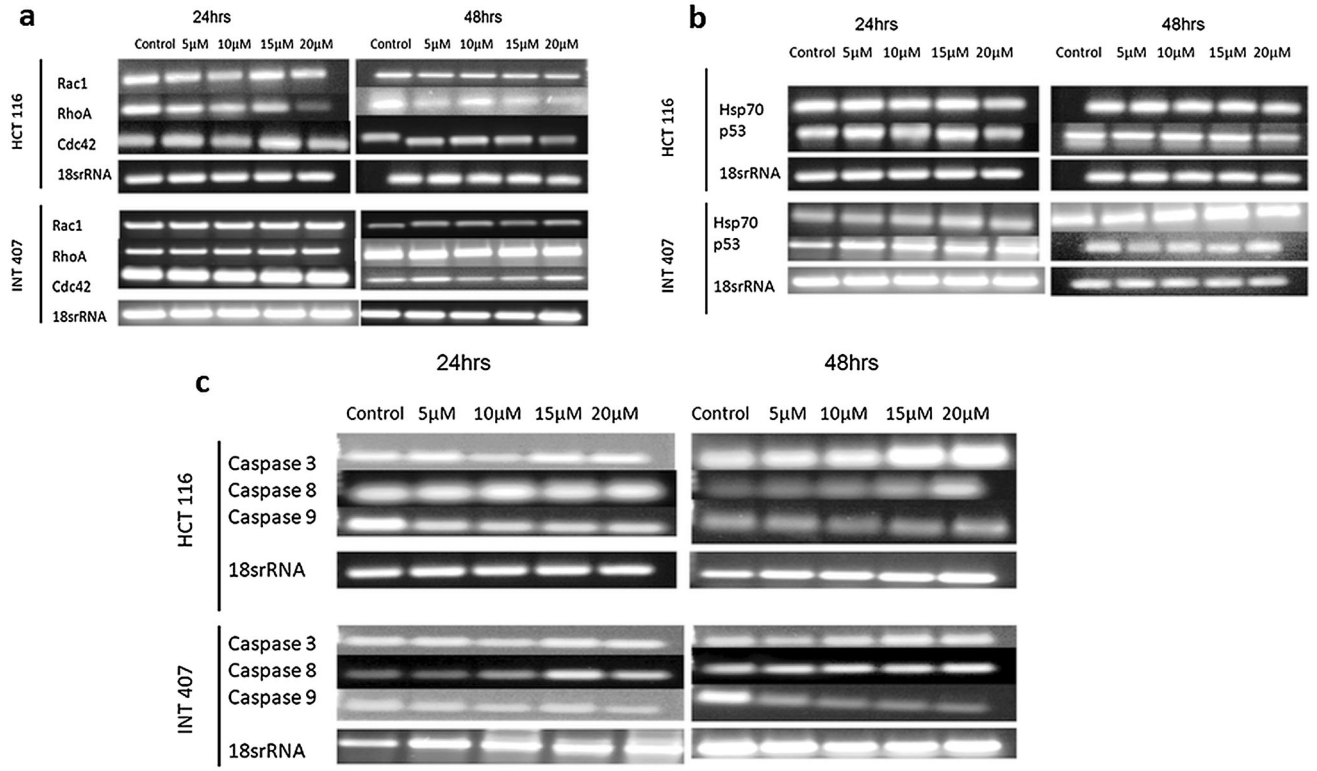

Figure 17. (**a**) Reverse Transcriptase PCR profile for Small GTPases gamete and 18srRNA of HCT 116 and INT 407 on incubation to varying concentrations of QC at 24 h (panel 1) and 48 h (panel 2). The first set of HCT 116 of Lane 1 is Positive Control, Lane 2 for 5 μM, Lane 3 for 10 μM, Lane 4 for 15 μM and Lane 5 for 20 μM for Panel 1 and Panel 2. Same for the second set, i.e., INT 407 cell line and lanes are the same, respectively. All experiments are run along with negative control, having no bands showing affirmation of the experiFment (not shown). (**b**). Reverse Transcriptase PCR profile for HSP 70 and p53comapred to 18srRNA of HCT 116 and INT 407 on incubation to varying concentrations of QC at 24 h (panel 1) and 48 h (panel 2). The first set of HCT 116 of Lane 1 is Positive Control, Lane 2 for 5 μM, Lane 3 for 10 μM, Lane 4 for 15 μM and Lane 5 for 20 μM for Panel 1 and Panel 2. Same for the second set, i.e., INT 407 cell line and lanes are the same, respectively. All experiments are run along with negative control, having no bands showing affirmation of the experiment. (**c**) Reverse Transcriptase PCR profile for caspase cascade relative to 18srRNA of HCT 116 and INT 407 on incubation to varying concentrations of QC at 24 h (panel 1) and 48 h (panel 2). The first set of HCT 116 of Lane 1 is Positive Control, Lane 2 for 5 μM, Lane 3 for 10 μM, Lane 4 for 15 μM and Lane 5 for 20 μM for Panel 1 and Panel 2. Same for the second set, i.e., INT 407 cell line and lanes are the same, respectively. All experiments are run along with negative control, having no bands showing affirmation of the experiment (not shown).

are initiator caspases and are expressed in extrinsic and intrinsic pathways, respectively (Jeong *et al.* 2011). Our study suggested that in both the cell lines, there has been a similar trend. Caspase 3, as well as caspase 8, is activated in both the cell lines, namely, HCT 116 and INT 407. The expression pattern of caspase 9 is reduced, which implies that cells in the presence of QC are executing themselves to apoptosis through the extrinsic pathway of apoptosis. Caspase 3 activation triggers the proteolytic cleavage of poly ADP-ribose polymerase resulting in DNA fragmentation, which is a common attribute of apoptosis (Hall 2009). When cytotoxicity increases, cells tend to trigger apoptosis by the extrinsic pathway (Ashkenazi 2008).

Although an analysis of results suggests that apoptosis is a mode of cell death, the complex process of cell death by QC allows a possibility of necrosis as well. Compared to the apoptosis observed in control cells, which were mostly in the early stage of apoptosis whereas, the treatment of QC at different concentrations showed an increased number of the early and late phases of apoptosis in both the cell lines. At the highest concentration of QC, there was a significant increase in the apoptotic nuclei in HCT 116 cell line having more than INT 407 cell line which constitutes both early and late stages. The percentage of necrosis was approximately constant at only a high level of QC in both the cell lines. Therefore, it might be inferred from the data that apoptosis was induced

by QC in both concentration and time-dependent manner (Xu *et al.* 2016). The cells after exposure to QC exhibited enhanced fragmentation or pyknosis of the chromatin, which is typical of cellular apoptosis (Grady and Carethers 2008; Wang *et al.* 2013).

Hsp70 prevents cell death by interfering with the ability of cytochrome c and Apaf-1 to recruit procaspase9 (Baskić *et al.* 2006). Hsp70 can block the release and activation of procaspase 9, which is functional for cell survival in terms of cell death (Evan *et al.* 1992). Our study implies that QC increases the Hsp70 expression in both the cell line HCT 116 and INT 407, downregulating caspase9 expressions. It is evident from the present study that Hsp70, the anti-apoptotic gene, is likely to block the expression of apoptosome by caspase 9 and hence not leading to apoptosis by the intrinsic pathway. In conclusion, our observation suggests that QC caused cytotoxicity in both cell lines. We emphasize that it has an inhibitory effect on essential steps of cancer progression, which includes migration, changes in the modulation of the cytoskeleton, cell to cell contact nuclear-cytoplasmic ratio. Downregulation of RhoA was documented in this study, a crucial regulator of cytoskeleton modulation. Its effects on multiple key signaling pathways, implicated in the malignant progression of numerous cancer types, make QC an exciting candidate as a chemotherapeutic agent in new types of combination treatments (Torres *et al.* 2013). Most importantly, cells were led to apoptosis, which was associated with caspase 3, caspase 8, and caspase 9. QC is an attractive chemotherapeutic agent having a 'shotgun' nature inducing different pathways leading to cell death, which opens a path to essential and interesting study in the future.

Acknowledgements

AS acknowledges the financial support for this work to DBT, India, as a pilot project grant [Grant No. 6242-P59/RGCB/PMD/DBT/ANSR/2015]. AS was supported by a fellowship from the same grant. The author acknowledges Prof. Utpal Roy for proofreading the manuscript.

References

Ashkenazi A 2008 Directing cancer cells to self-destruct with pro-apoptotic receptor agonists. *Nat. Rev. Drug Discov.* **7** 1001

Baskić D, Popović S, Ristić P and Arsenijević NN 2006 Analysis of cycloheximide-induced apoptosis in human leukocytes: Fluorescence microscopy using annexin V/propidium iodide versus acridin orange/ethidium bromide. *Cell Biol. Int.* **30** 924–932

Celisa Santimano M, Martin A, Kowshik M and Sarkar A 2013 Zinc oxide nanoparticles cause morphological changes in human A549 cell line through alteration in the expression pattern of small GTPases at mRNA level. *J. Bionanosci.* **7** 300–306

Cheng YT, Lin JA, Jhang JJ and Yen GC 2019 Protocatechuic acid-mediated DJ-1/PARK7 activation followed by PI3K/mTOR signaling pathway activation as a novel mechanism for protection against ketoprofen-induced oxidative damage in the gastrointestinal mucosa. *Free Radic. Biol.* **130** 35–47

Chowdhury I, Tharakan B and Bhat GK 2006 Caspases—an update. *Comp. Biochem. Phys. B Biochem. Mol Bio*. **151** 10–27

de Lira Mota KS, Dias GEN, Pinto MEF, Luiz Ferreira Â, Monteiro Souza-Brito AR, Hiruma-Lima CA, Barbosa-Filho JM and Batista LM 2009 Flavonoids with gastroprotective activity. *Molecules* **14** 979–1012

Ehsanian R, Van Waes C and Feller SM 2011 Beyond DNA binding-a review of the potential mechanisms mediating quinacrine's therapeutic activities in parasitic infections, inflammation, and cancers. *Cell Commun. Signal.* **9** 13

Evan GI, Wyllie AH, Gilbert CS, Littlewood TD, Land H, Brooks M, Waters CM, Penn LZ and Hancock DC 1992 Induction of apoptosis in fibroblasts by c-myc protein. *Cell* **69** 119–128

Fasanmade AA, Owuor ED, Ee RP, Qato D, Heller M and Kong ANT 2001 Quinacrine induces cytochrome c-dependent apoptotic signaling in human cervical carcinoma cells. *Arch. Pharm. Res.* **24** 126–135

Friedl P and Wolf K 2003 Tumour-cell invasion and migration: diversity and escape mechanisms. *Nat. Rev. Cancer* **3** 362

Fritz G, Just I and Kaina B 1999 Rho GTPases are overexpressed in human tumors. *Int. J. Cancer.* **81** 682–687

Goodell JR, Ougolkov AV, Hiasa H, Kaur H, Remmel R, Billadeau DD and Ferguson DM 2008 Acridine-based agents with topoisomerase II activity inhibit pancreatic cancer cell proliferation and induce apoptosis. *J. Med. Chem.* **51** 179–182

Grady WM and Carethers JM 2008 Genomic and epigenetic instability in colorectal cancer pathogenesis. *Gastroenterology* **135** 1079–1099

Gupta SK, Croffie JM, Pfefferkorn MD and Fitzgerald JF 2003 Diagnostic yield of duodenal aspirate for G. lamblia and comparison to duodenal mucosal biopsies. *Dig. Dis. Sci.* **48** 605–607

Gurova KV, Hill JE, Guo C, Prokvolit A, Burdelya LG, Samoylova E, Khodyakova AV, Ganapathi R, Ganapathi M, Tararova ND and Bosykh D 2005 Small molecules

that reactivate p53 in renal cell carcinoma reveal a NF-κB-dependent mechanism of p53 suppression in tumors. *Proc. Natl. Acad. Sci. USA* **102** 17448–17453

Gurova K 2009 New hopes from old drugs: revisiting DNA-binding small molecules as anticancer agents. *Futur. Oncol.* **5** 1685–1704

Hall A 2009 The cytoskeleton and cancer. *Cancer Metastasis Rev.* **28** 5–14

Harikumar KB, Kuttan G and Kuttan R 2009 Phyllanthus amarus inhibits cell growth and induces apoptosis in Dalton's lymphoma ascites cells through activation of caspase-3 and downregulation of Bcl-2. *Integr. Cancer Ther.* **8** 190–194

Jemal A, Bray F, Center MM, Ferlay J, Ward E and Forman D 2011 Global cancer statistics. *CA Cancer J. Clin.* **61** 69–90

Jeong HS, Choi Y, Lee ER, Kim JH, Jeon K, Lee HJ and Cho SG. 2011. Involvement of caspase-9 in autophagy-mediated cell survival pathway. *Biochim. Biophys. Acta Mol. Cell Res.* **1813** 80–90

Jin Z and El-Deiry WS 2005 Overview of cell death signaling pathways. *Cancer. Biol. Ther.* **4** 147–171

Kominami K, Nakabayashi J, Nagai T, Tsujimura Y, Chiba K, Kimura H, Miyawaki A, Sawasaki T, Yokota H, Manabe N and Sakamaki K 2012 The molecular mechanism of apoptosis upon caspase-8 activation: Quantitative experimental validation of a mathematical model. *Biochim. Biophys. Acta Mol. Cell Res.* **1823** 1825–1840

Lalitha P, Veena V, Vidhyapriya P, Lakshmi P, Krishna R and Sakthivel N 2016 Anticancer potential of pyrrole (1, 2, a) pyrazine 1, 4, dione, hexahydro 3-(2-methyl propyl) (PPDHMP) extracted from a new marine bacterium, Staphylococcus sp. strain MB30. *Apoptosis* **21** 566–577

Lozano E, Betson M and Braga VM 2003 Tumor progression: small GTPases and loss of cell–cell adhesion. *Bioessays* **25** 452–463

Maity P, Biswas K, Roy S, Banerjee RK and Bandyopadhyay U 2003 Smoking and the pathogenesis of gastroduodenal ulcer–recent mechanistic update. *Mol. Cell. Biochem.* **253** 329–338

Moghaddam DD, Ghadirian E and Azami M 2005 Blastocystis hominis and the evaluation of efficacy of metronidazole and trimethoprim/sulfamethoxazole. *Parasitol. Res*. **96** 273–275

Ortega YR and Adam RD 1997 Giardia: overview and update. *Clin. Infect. Dis.* **25** 545–549

Pancione M, Remo A and Colantuoni V 2012 Genetic and epigenetic events generate multiple pathways in colorectal cancer progression. *Patholog. Res. Int.* **2012** 11

Paul-Samojedny M, Kokocińska D, Samojedny A, Mazurek U, Partyka R, Lorenz Z and Wilczok T 2005 Expression of cell survival/death genes: Bcl-2 and Bax at the rate of colon cancer prognosis *Biochim. Biophys. Acta Mol. Basis Dis.* **1741** 25–29

Pertz O, Hodgson L, Klemke RL and Hahn KM 2006 Spatiotemporal dynamics of RhoA activity in migrating cells. *Nature* **440** 1069

Preet R, Mohapatra P, Mohanty S, Sahu SK, Choudhuri T, Wyatt MD and Kundu CN 2012 Quinacrine has anticancer activity in breast cancer cells through inhibition of topoisomerase activity. *Int. J. Cancer* **130** 1660–1670

Sander EE, van Delft S, Jean P, Reid T, van der Kammen RA, Michiels F and Collard JG 1998 Matrix-dependent Tiam1/Rac signaling in epithelial cells promotes either cell–cell adhesion or cell migration and is regulated by phosphatidylinositol 3-kinase. *J. Cell Biol.* **143** 1385–1398

Sarkar A, Parikh N, Hearn SA, Fuller MT, Tazuke SI and Schulz C 2007 Antagonistic roles of Rac and Rho in organizing the germ cell microenvironment. *Curr. Biol.* **17** 1253–1258

Tahir AA, Sani NFA, Murad NA, Makpol S, Ngah WZW and Yusof YAM 2015 Combined ginger extract & Gelam honey modulate Ras/ERK and PI3K/AKT pathway genes in colon cancer HT29 cells. *Nutr. J.* **14** 31

Torres RE M, Banegas EI, Mendoza M, Diaz C, Bucheli ST M, Fontecha GA, Alam MT, Goldman I, Udhayakumar V and Zambrano JON 2013 Efficacy of chloroquine for the treatment of uncomplicated *Plasmodium falciparum* malaria in Honduras. *Am. J. Trop. Med. Hyg.* **88** 850–854

Upcroft P and Upcroft JA 2001 Drug targets and mechanisms of resistance in the anaerobic protozoa *Clin. Micro. Revs*. **14** 150–164

Van Hengel J, D'Hooge P, Hooghe B, Wu X, Libbrecht L, De Vos R, Quondamatteo F, Klempt M, Brakebusch C and Van Roy F 2008 Continuous cell injury promotes hepatic tumorigenesis in cdc42-deficient mouse liver. *Gastroenterology* **134** 781–792

Wang G, Wang X, Yu H, Wei S, Williams N, Holmes DL, Halfmann R, Naidoo J, Wang L, Li L and Chen S 2013 Small-molecule activation of the TRAIL receptor DR5 in human cancer cells. *Nat. Chem. Biol.* **9** 84

Wiezorek J, Holland P and Graves J 2010 Death receptor agonists as a targeted therapy for cancer. *Clin. Cancer Res.* **16** 1701–1708

Xu YQ, Zhang JH and Yang XS 2016 Corosolic acid induces potent anti-cancer effects in CaSki cervical cancer cells through the induction of apoptosis, cell cycle arrest and PI3K/Akt signalling pathway. *Bangladesh J. Pharmacol.* **11** 453–459

Corresponding editor: Sorab Dalal